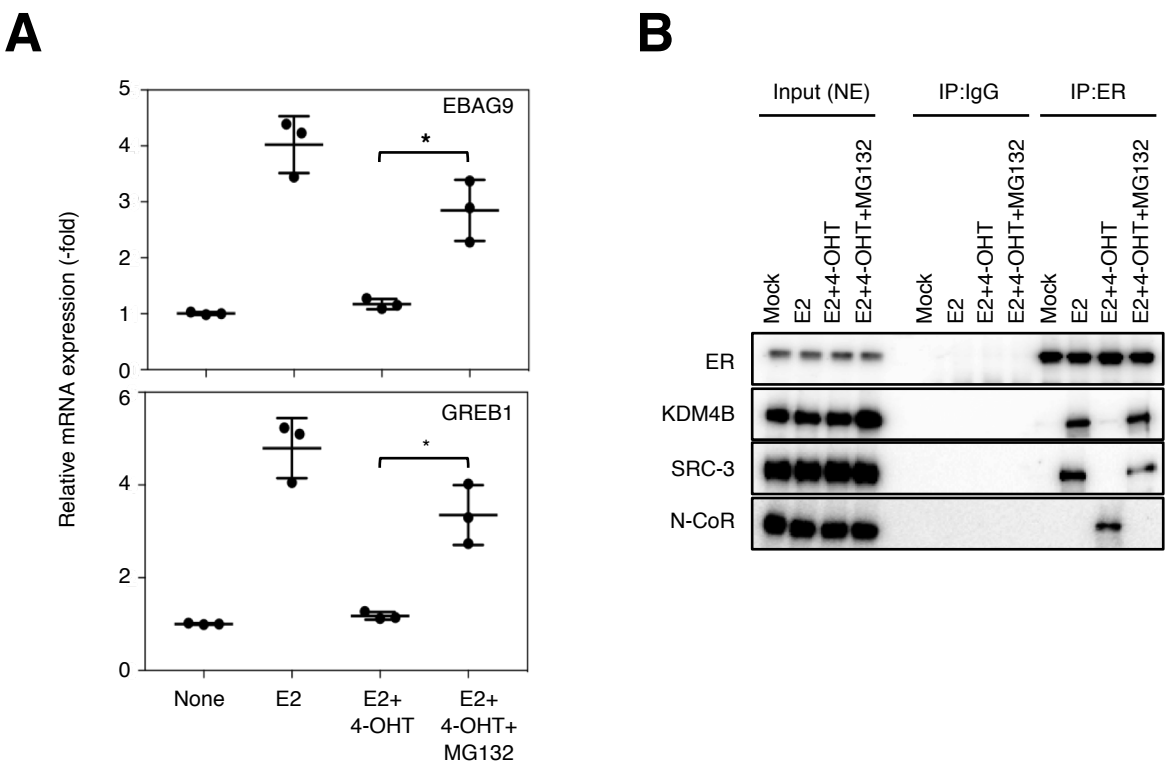

Supplementary Figure 1. Proteasome-dependent protein degradation is required for proper shutdown of E2-signaling by 4-OHT in T47D cells

(A) T47D cells starved of E2 for 72 hrs were cultured with medium containing E2 (10 nM) for 6 hrs and then incubated in medium containing 4-OHT (100 nM) with or without MG132 (10 μg/ml) for 12 hrs. Total RNA from the treated cells was subjected to qPCR analysis. The data are presented as the means ±s.d. of three independent experiments. *p<0.01, ***p<0.005 **(B)** The nuclear extracts (NE) of cells treated as in **(A)** were immunoprecipitated using the indicated antibodies and subjected to immunoblotting.

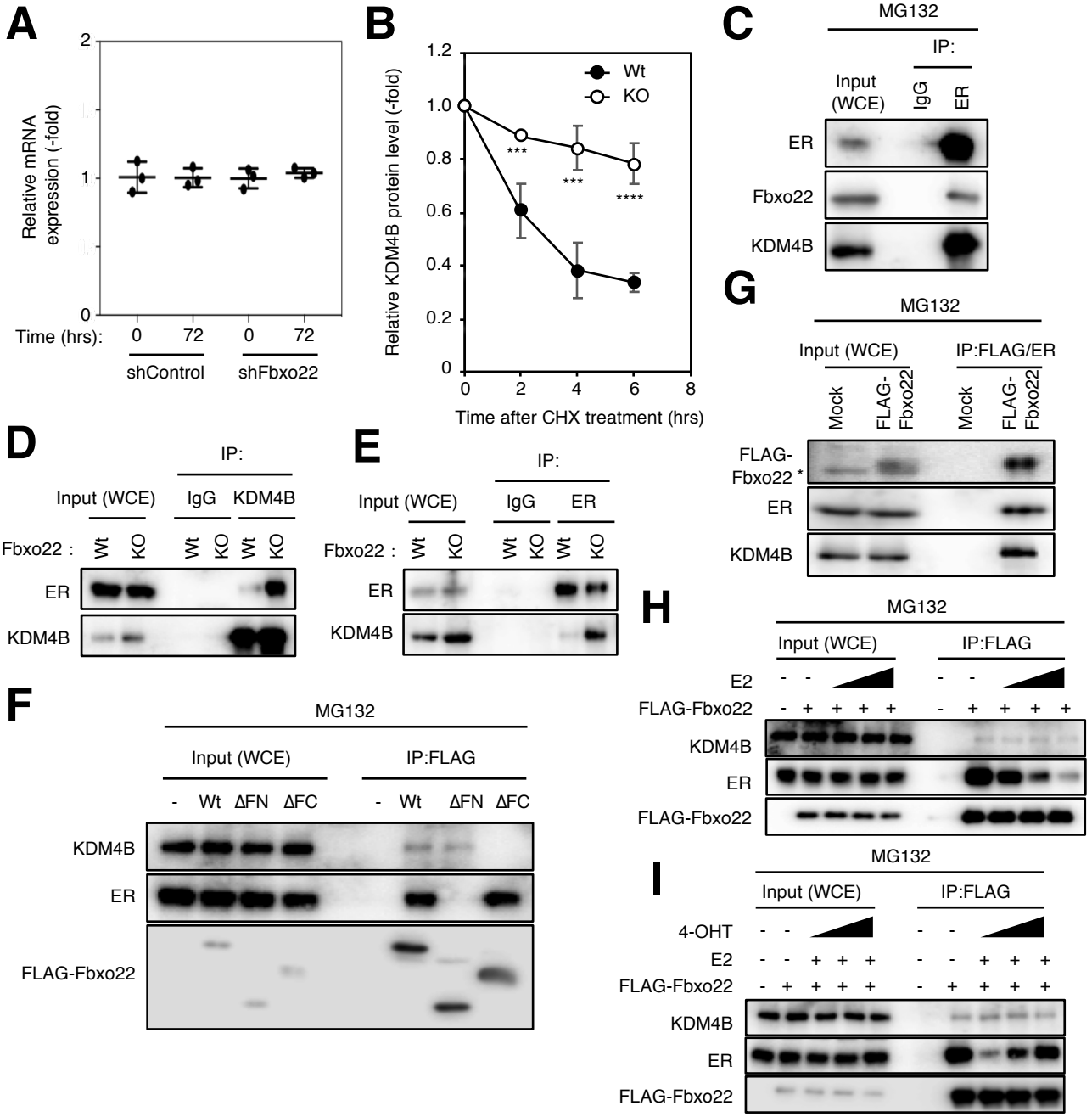

Supplementary Figure 2. Fbxo22 forms a ternary complex with ER and KDM4B in a ligand type-dependent manner in T47D cells

(A) The indicated Dox-shRNAs-MCF-7 cells were treated with doxycycline (1 μg/ml). Total RNA from the treated cells at the indicated times was subjected to qPCR analysis. The data are presented as the means ±s.d. of three independent experiments. **(B)** Wild-type (Wt) or Fbxo22-KO (KO) T47D cells were analyzed as in Figure 2B. **(C)** T47D cells were analyzed as in Figure 2D. **(D)(E)** Wild-type (Wt) or Fbxo22-KO (KO) T47D cells were analyzed as in Figure 2E and 2F. **(F)** Dox-wild-type FLAG-Fbxo22 (Wt) or mutants lacking FIST-N (ΔFN) or FIST-C (ΔFC) T47D cells were analyzed as in Figure 2G. **(G)** Dox-FLAG-Fbxo22-T47D cells were analyzed as in Figure 2H. **(H)(I)** Dox-FLAG-Fbxo22-T47D cells were analyzed as in Figure 2I and 2J.

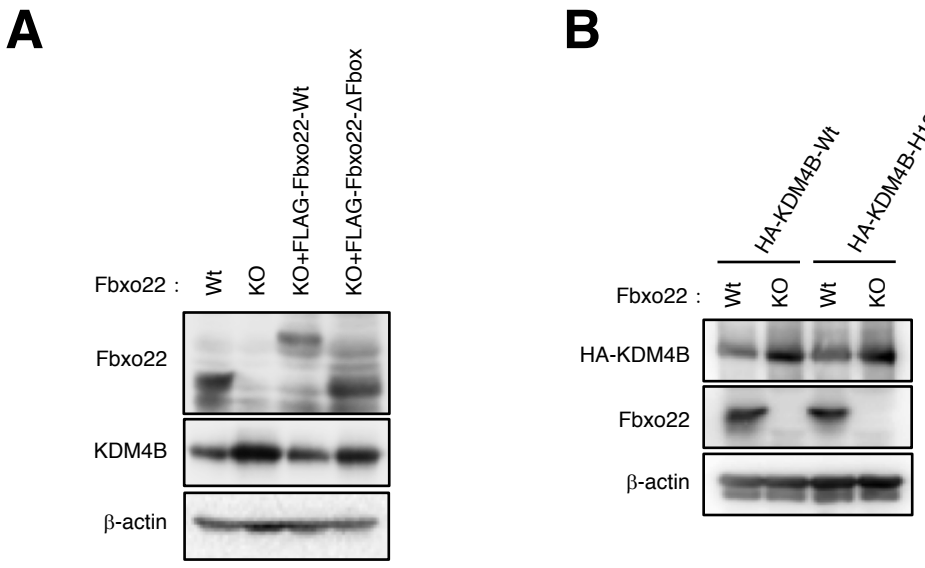

Supplementary Figure 3. SCF^{Fbxo22}-dependent regulation of KDM4B stability requires the F-box of Fbxo22, but not catalytic activity of KDMA4B

(A) Lysates from wild-type (Wt), Fbxo22 KO (KO), and KO T47D cells expressing Fbxo22-wild type (Fbxo22-Wt) or its mutant lacking the F-box (ΔFbox) were subjected to immunoblotting using the indicated antibodies. **(B)** Lysates from Wt or KO T47D cells expressing wild-type HA-KDM4B (HA-KDM4B-Wt) or its catalytic mutant (HA-KDM4B-H189A) were subjected to immunoblotting using the indicated antibodies.

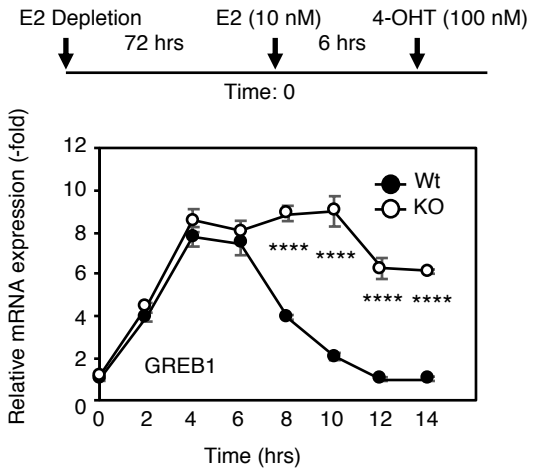

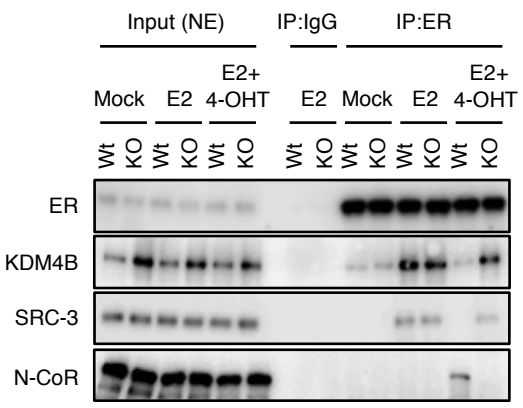

Supplementary Figure 4. Antagonistic activity of 4-OHT requires Fbxo22 in T47D cells

(A) The experimental outline is shown (upper panel). Wild-type (Wt) or Fbxo22 KO (KO)T47D cells were starved of E2 for 72 hrs, treated with E2 (10 nM) for 6 hrs, and then treated with 4-OHT (100 nM). Total RNA from the treated cells at the indicated times was subjected to qPCR analysis. The data are presented as the means ±s.d. of three independent experiments. ****p<0.001 **(B)** The nuclear extracts (NE) from cells treated as in (A) at 12 hrs were immunoprecipitated using the indicated antibodies and subjected to immunoblotting.

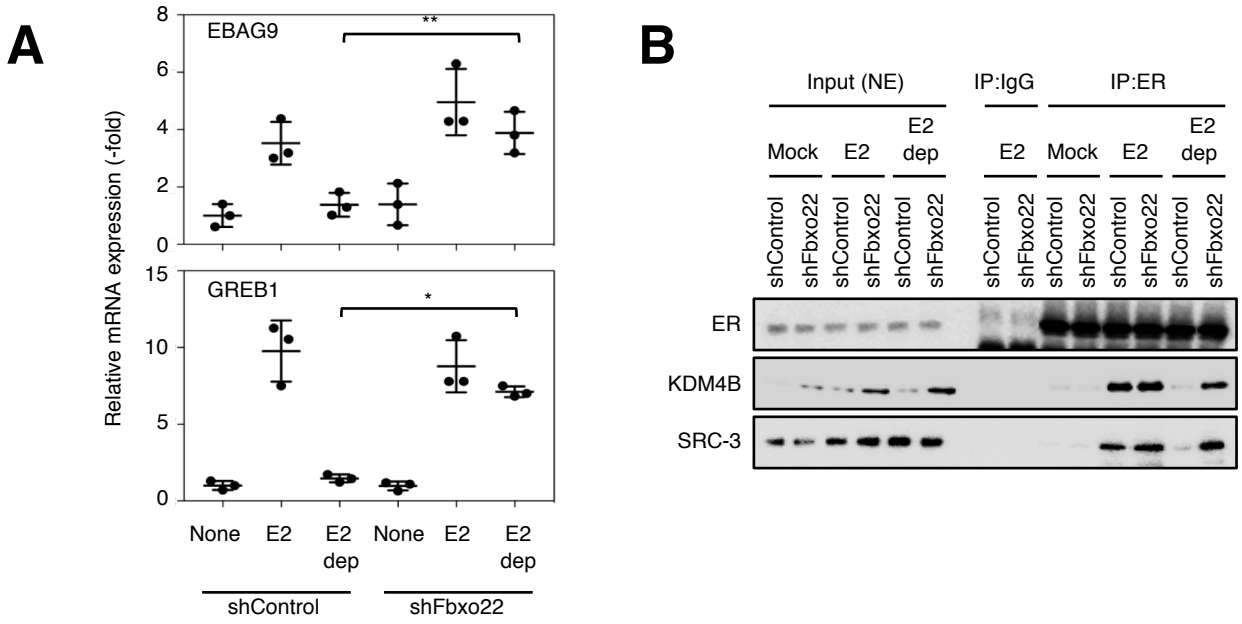

Supplementary Figure 5. Fbxo22 is essential for suppression of ER transcription and coactivator release from ER by E2 depletion

(A) The indicated Dox-shRNAs-MCF-7 cells were starved of E2 in the presence of doxycycline (1 μg/ml) for 72 hrs, treated with E2 (10 nM) for 6 hrs, and then depleted of E2 for 24 hrs. Total RNA from the treated cells was subjected to qPCR analysis. The data are presented as the means ±s.d. of three independent experiments. *$p<0.01$, **$p<0.05$ **(B)** The nuclear extracts (NE) from cells treated as described in **(A)** were immunoprecipitated using the indicated antibodies and subjected to immunoblotting.

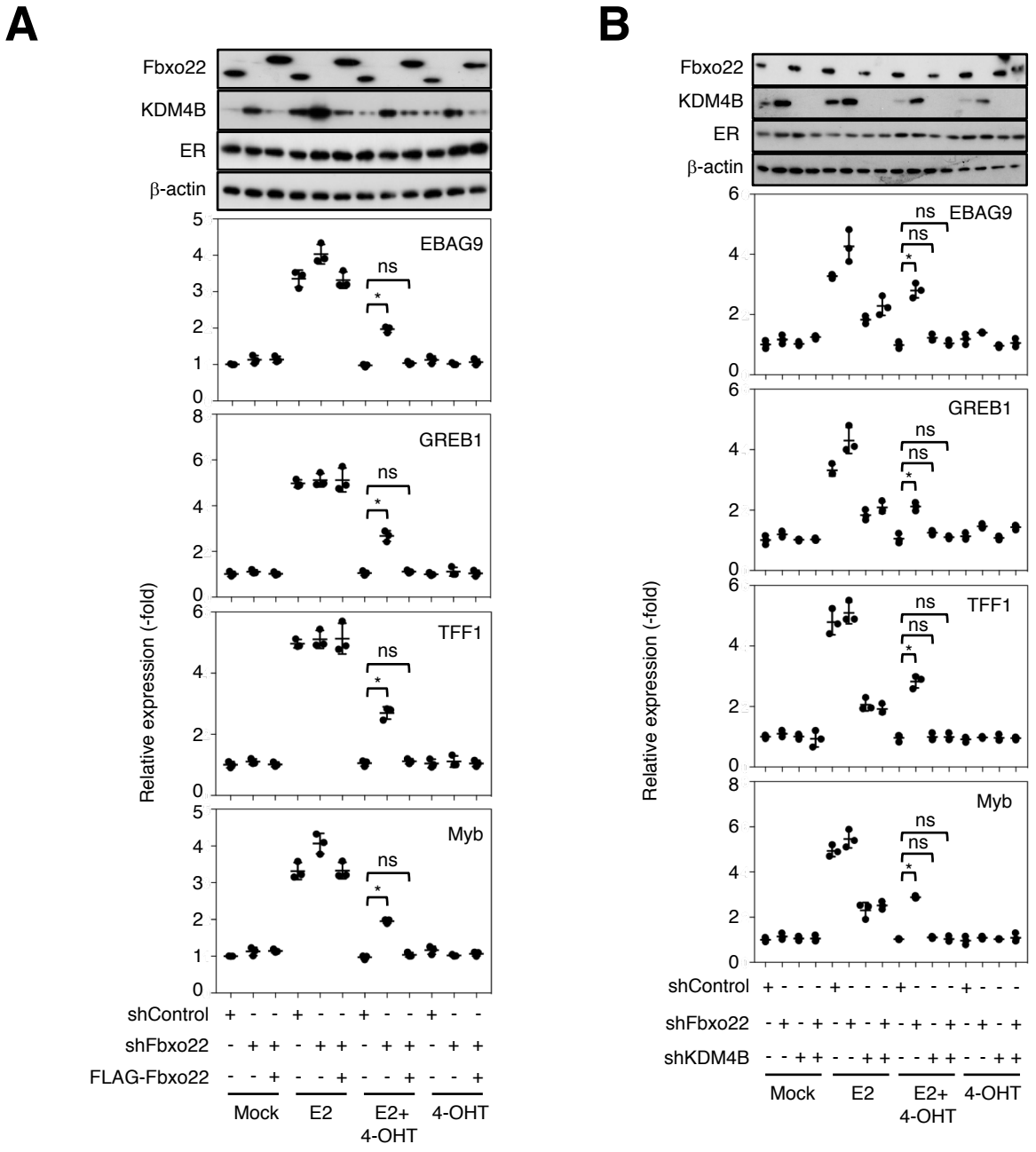

Supplementary Figure 6. SCF^{Fbxo22}-mediated degradation of KDM4B complexed with ER is essential for the antagonistic action of 4-OHT

(A) The indicated Dox-shRNAs-MCF-7 cells expressing FLAG-Fbxo22 were starved of E2 in the presence of doxycycline (1 μg/ml) for 72 hrs, and then treated with E2 (10 nM) in the presence or absence of 4-OHT (100 nM) for 6 hrs. The lysates from the treated cells were immunoprecipitated using the indicated antibodies and subjected to immunoblotting. Total RNA from the treated cells was subjected to qPCR analysis. The data are presented as the means ±s.d. of three independent experiments. *p<0.01, **p<0.05 **(B)** The indicated Dox-shRNAs-MCF-7 cells were treated and analyzed as in **(A)**. *p<0.01, **p<0.05, ***p<0.005, ns: not significant

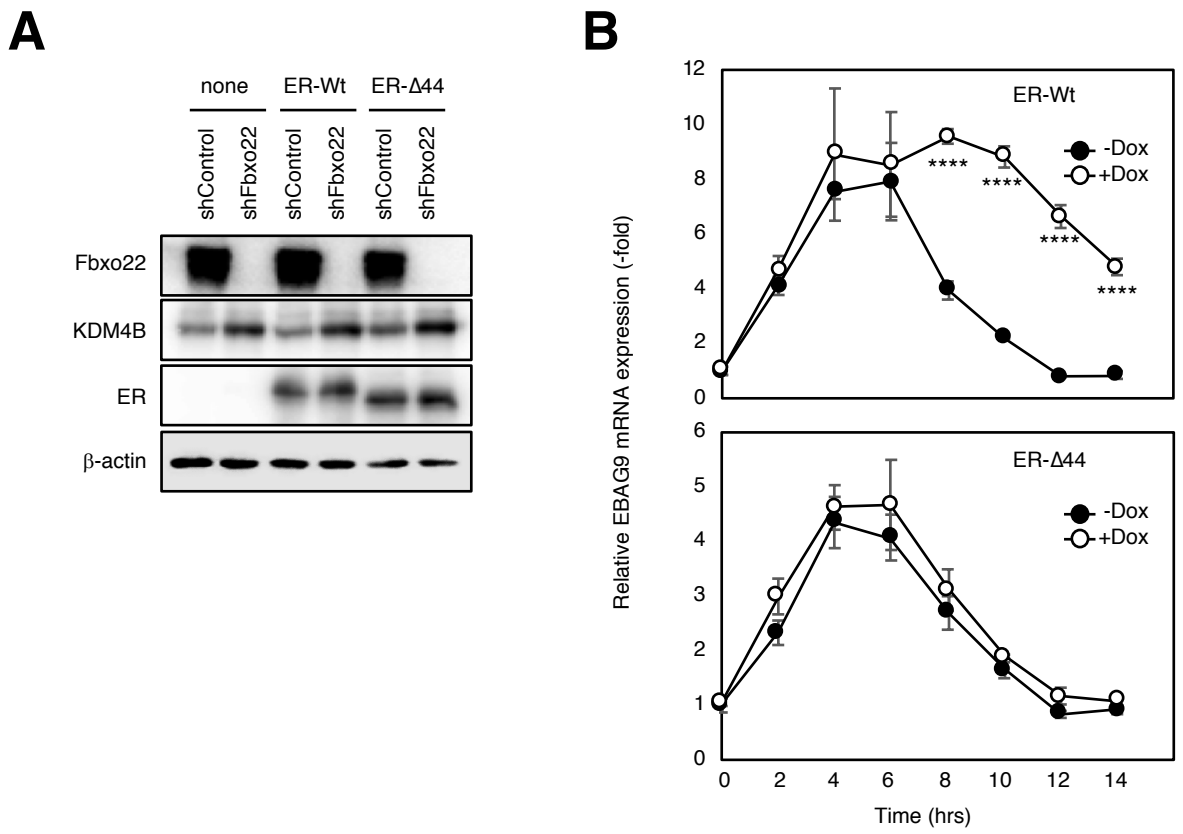

Supplementary Figure 7. ER-induced EBAG9 transcription in Fbxo22-depleted cells in the presence of 4-OHT depends on AF1 activity

(A) U2OS cells expressing wild-type ER or its Δ44 mutant were starved of E2 in the presence of doxycycline (1 μg/ml) for 72 hrs. Cells were then harvested and the lysates were subjected to immunoblotting using the indicated antibodies. **(B)** U2OS cells expressing wild-type ER or its Δ44 mutant were starved of E2 in the presence of doxycycline (1 μg/ml) for 72 hrs, treated with E2 (10 nM) for 6 hrs, and then treated with 4-OHT (100 nM). Total RNA from treated cells at the indicated times was subjected to qPCR analysis. The data are presented as the means ±s.d. of three independent experiments. ****p<0.001

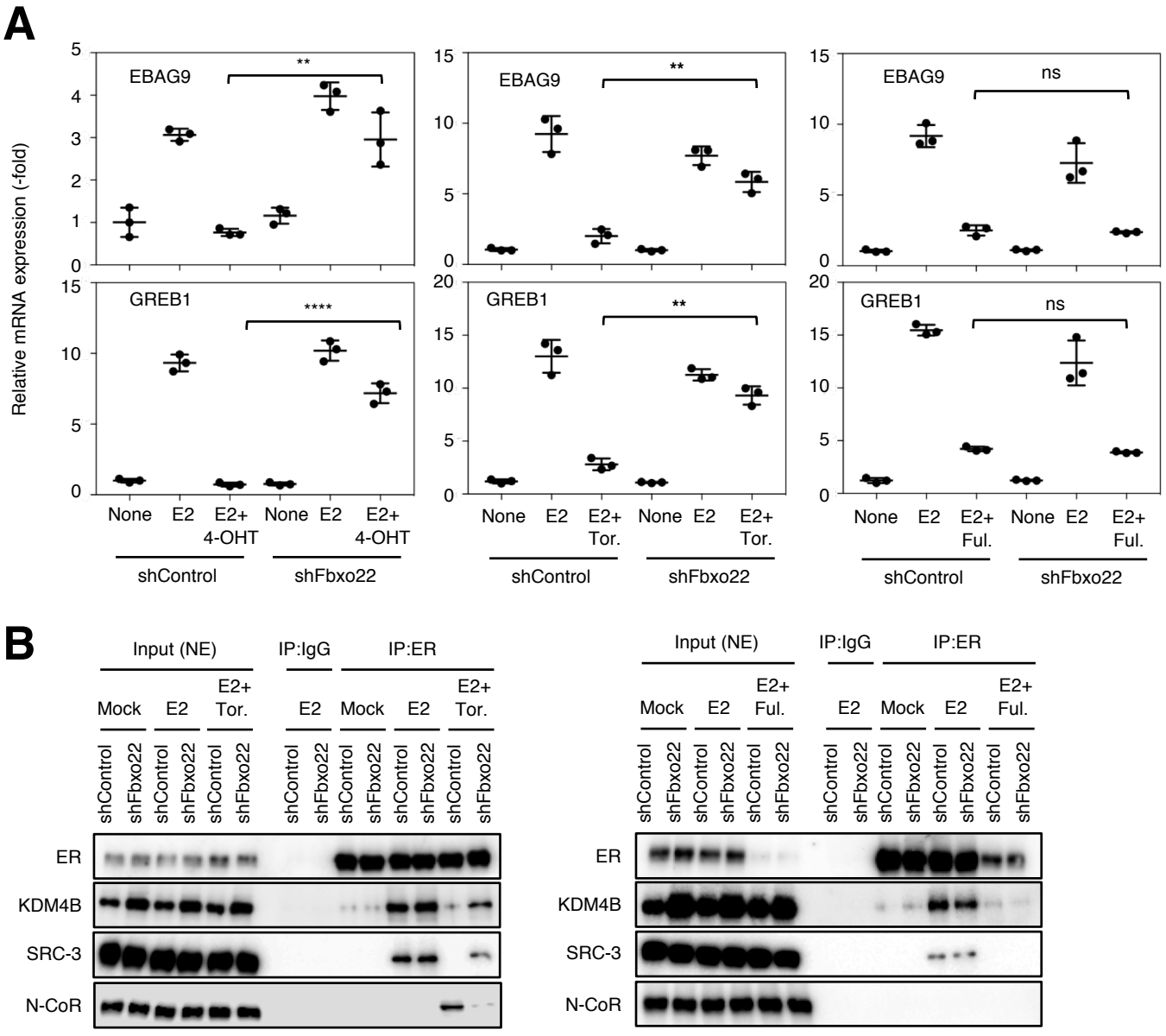

Supplementary Figure 8. SCF^{Fbxo22}-mediated degradation of KDM4B complexed with ER is essential for the antagonistic action of toremifene, but not fulvestrant

(A) The indicated Dox-shRNAs-MCF-7 cells were starved of E2 in the presence of doxycycline (1 μg/ml) for 72 hrs, treated with E2 (10 nM) for 6 hrs, and then treated with 4-OHT (100 nM), toremifene (Tor.: 100 nM), or fulvestrant (Ful.: 100 nM) for 12 hrs. Total RNA from treated cells was subjected to qPCR analysis. The data are presented as the means ±s.d. of three independent experiments. **p<0.01, ****p<0.001, ns: not significant **(B)** The nuclear extracts (NE) from cells treated as described in **(A)** were immunoprecipitated using the indicated antibodies and subjected to immunoblotting.

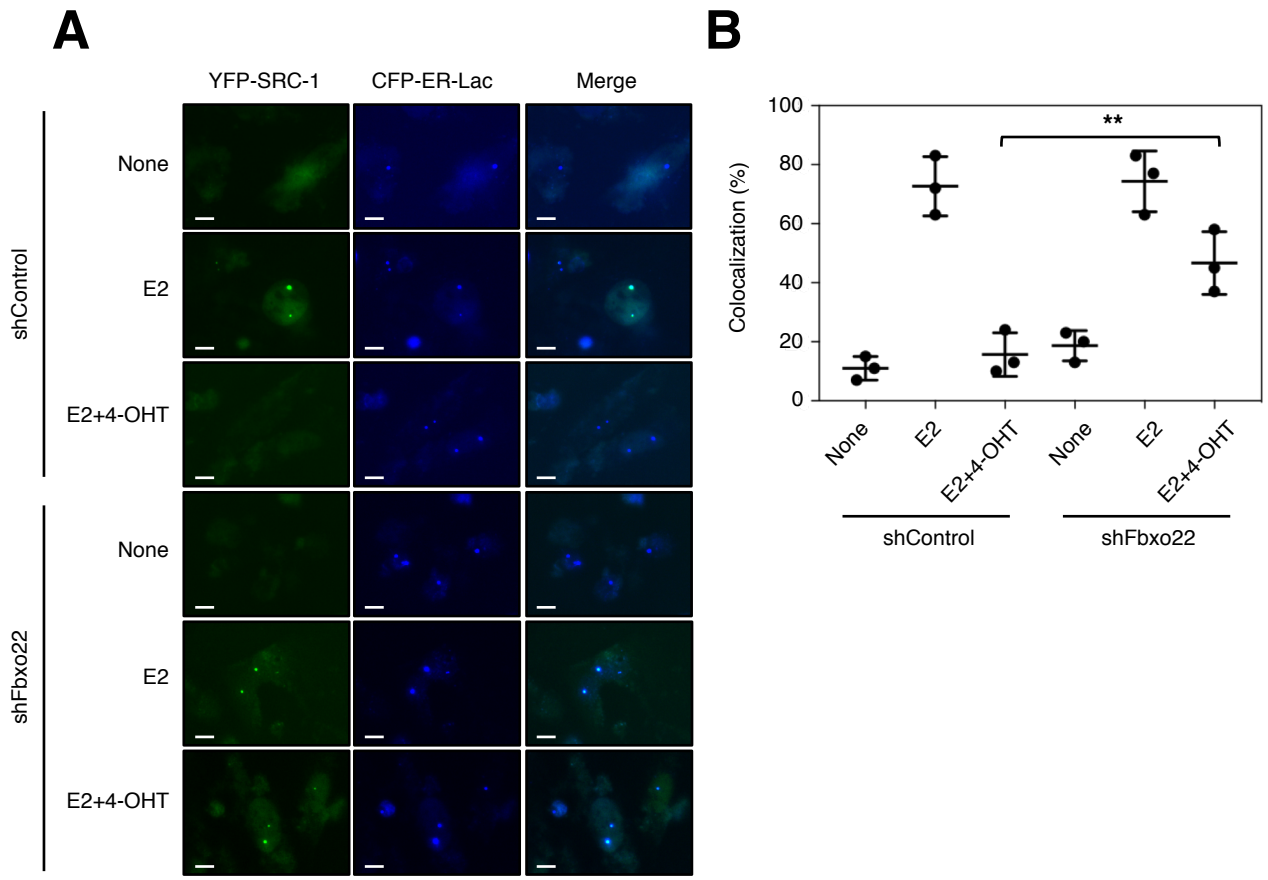

Supplementary Figure 9. The real-time cellular dynamics of ER-SRC-1 complexes reveals the essential role of Fbxo22 in SRC-1 release from ER in the presence of 4-OHT

(A) U2OS-LacO-I-SceI-TetO cells expressing the Dox-inducible shControl or shFbxo22 were transfected with YFP-SRC-1 and CFP-ERalpha-Lac plasmids, followed by treatment with doxycycline (1 μg/ml) in E2-depleted medium for 72 hrs. These cells were then treated with or without E2 (10 nM) and/or 4-OHT (100 nM) for 2 hrs and fixed with 4% formaldehyde. Representative images of CFP-ERalpha-Lac foci and YFP-SRC-1 foci are shown. Scale bar. 10 μm. **(B)** The number of cells positive for colocalization of CFP-ERalpha-Lac foci and YFP-SRC-1 foci as in **(A)** were counted. The data are presented as the means ±s.d. of three independent experiments.

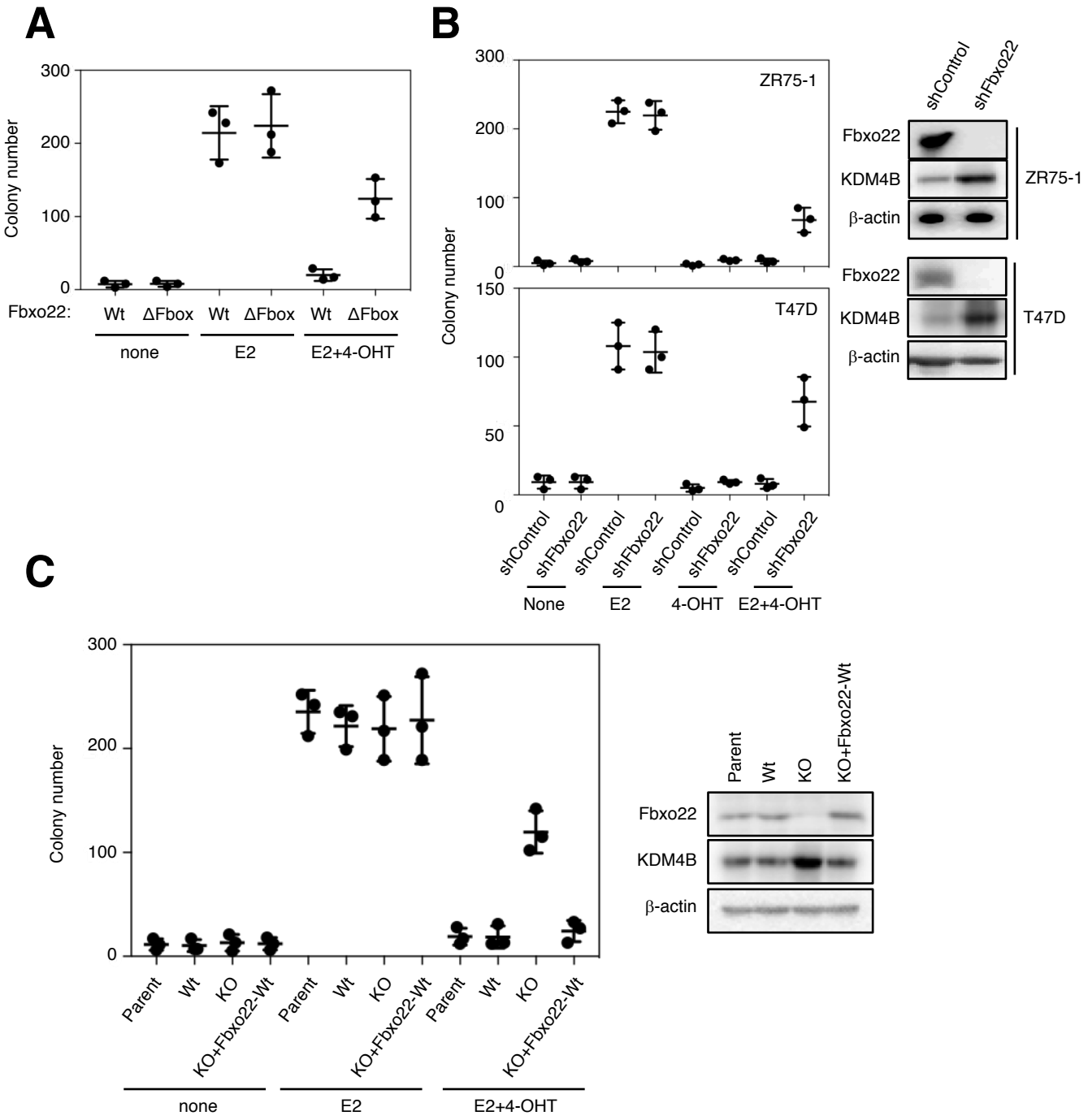

Supplementary Figure 10. Fbxo22 is required for the antagonistic activity of TAM in ZR75-1 and T47D cells

(A) KO T47D cells expressing Fbxo22-Wt or Fbxo22-ΔFbox were starved of E2 for 72 hrs and then analyzed as in Figure 7A. Data are shown as means ±SD of at three independent experiments. **(B)** The indicated shRNAs-ZR75-1 or -T47D cells were starved of E2 and analyzed as in **(A)** (left panels). Lysates of the cells in E2-depleted medium containing doxycycline (1 μg/ml) for 72 hrs were subjected to immunoblotting using the indicated antibodies (right panels). **(C)** Parental**,** wild-type (Wt), Fbxo22-KO (KO), or KO expressing wild-type Fbxo22 (KO+Fbxo33-Wt) T47D cells were starved in E2-depleted medium for 72 hrs and then analyzed as in **(A)**.

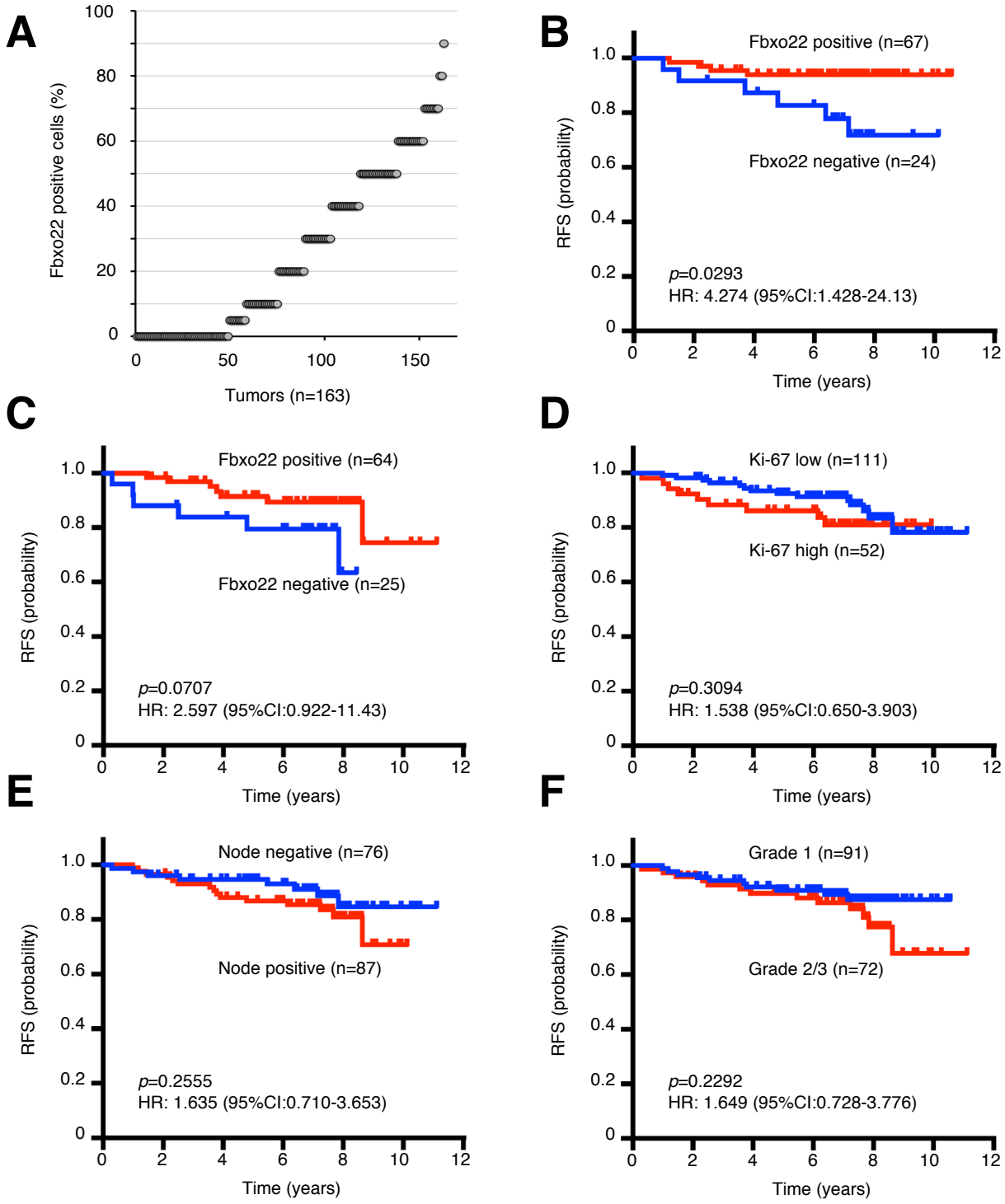

Supplementary Figure 11. Distribution of Fbxo22 positivity and RFS stratified by Fbxo22 expression in separate cohorts or by other clinicopathological factors

(A) The distribution of the percentage of Fbxo22-positive cells in 163 ER-positive/HER2-negative breast cancer cases is shown. RFS stratified by Fbxo22 protein expression in grade 1 ER-positive/HER2-negative breast cancers **(B)** and in tamoxifen-untreated breast cancers **(C)**. RFS stratified by Ki-67 status (≦10% vs 20%≦) **(D)**, node status (positive vs negative) **(E)** or grade (1 vs 2/3) **(F)** in all T2 ER-positive/HER2-negative breast cancers. Kaplan-Meyer survival curves are shown. P values and hazard ratios were calculated using a log-rank test.

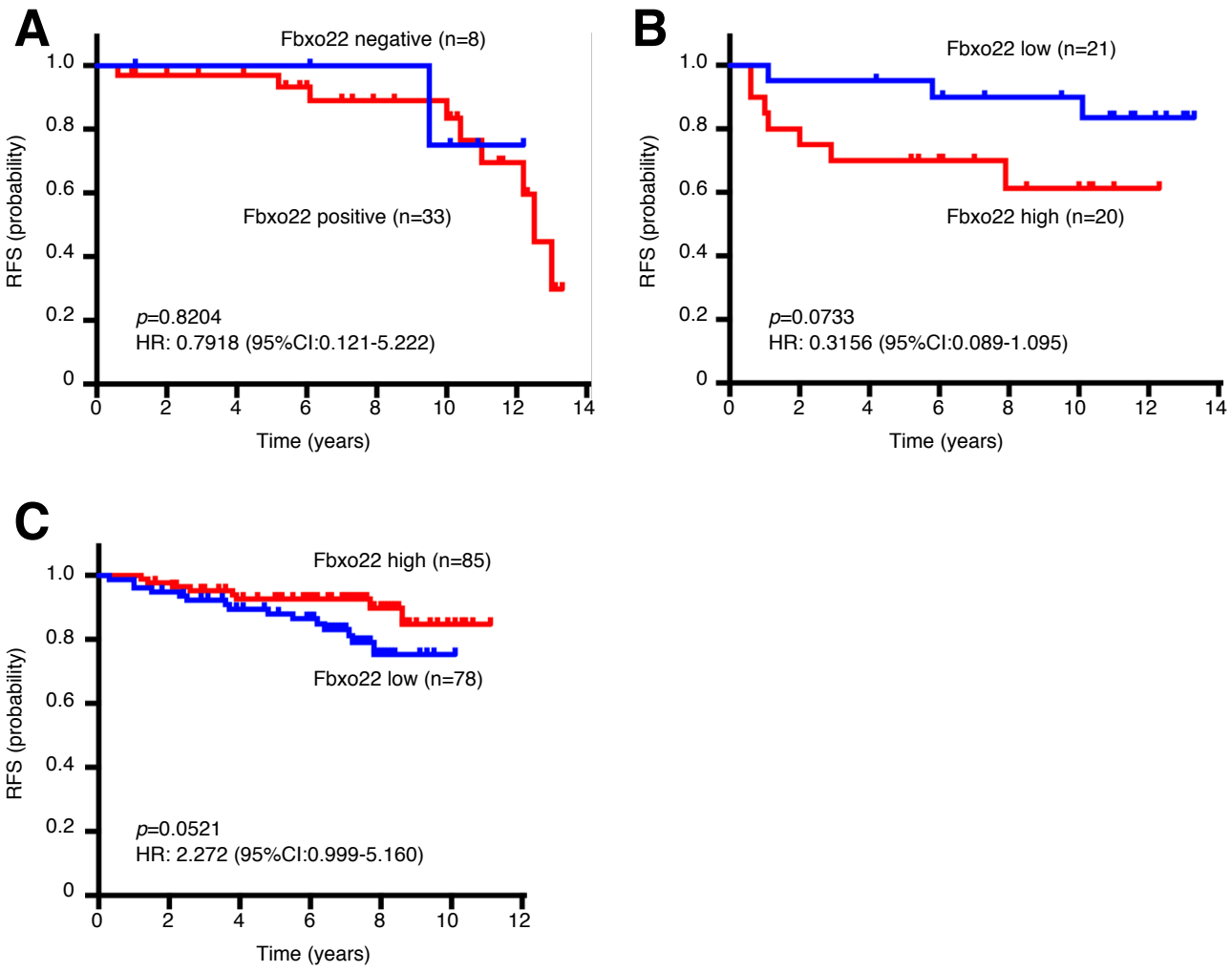

Supplementary Figure 12. Low protein expression level of Fbxo22 does not associate with a poor outcome in patients with ER-negative breast cancers

(A and B) RFS stratified by positivity (negative, < 1% vs positive, 1% ≦) **(A)** or the median cutoff point (low, < 50% vs high, 50% ≦) **(B)** of Fbxo22 protein expression in T2 ER-negative breast cancers. **(C)** RFS stratified by the median cutoff point (low, < 20% vs high, 20% ≦) in the main cohort of ER-positive/HER2-negative breast cancers is also shown for comparison. Kaplan-Meyer survival curves are shown. P values and hazard ratios were calculated using a log-rank test. Clinicopathological variables of the ER-negative breast cancer patients are listed in Table S4.

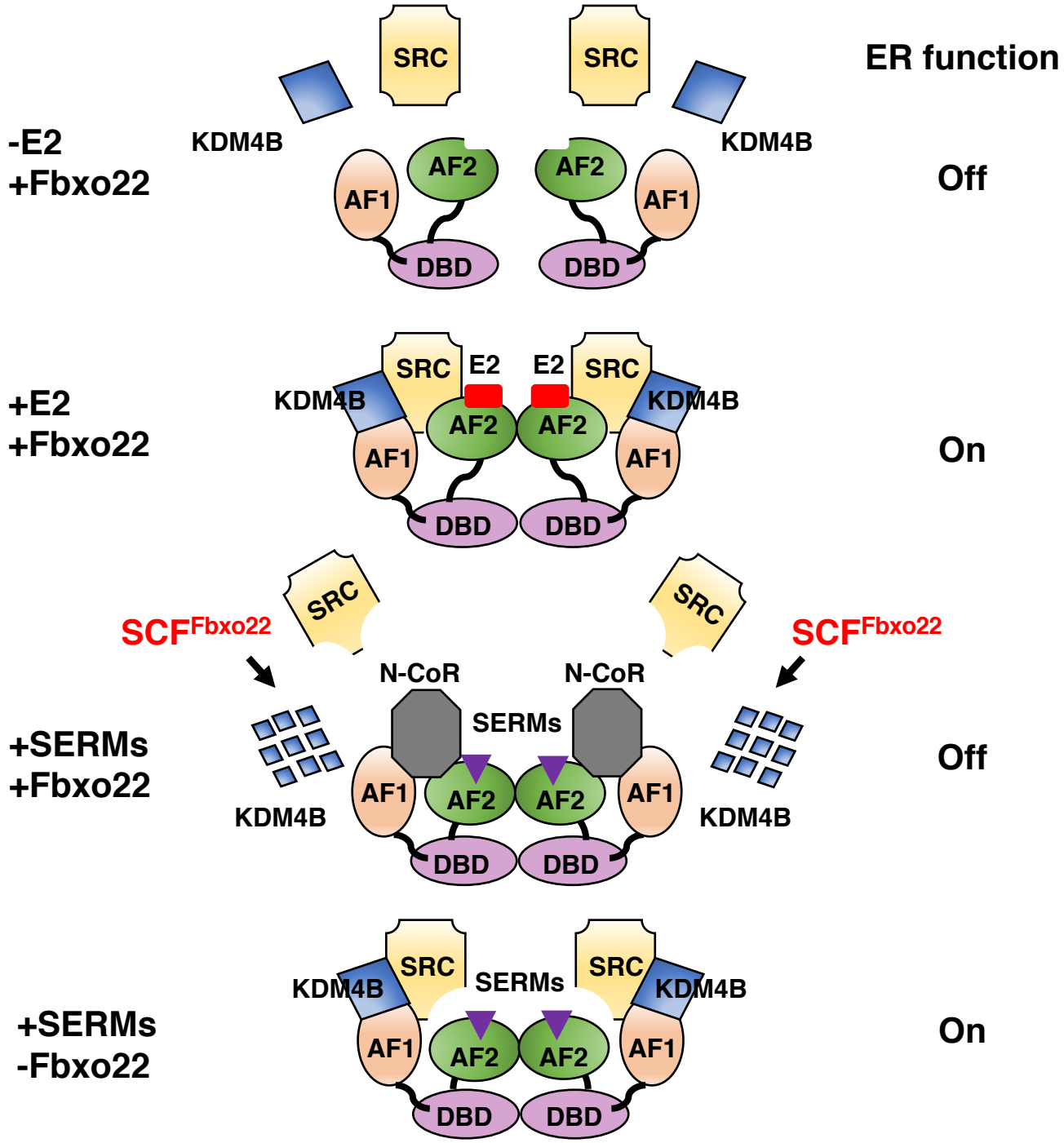

Supplementary Figure 13. Scheme of Fbxo22 function in cofactor dynamics on ER in the presence of E2 or SERMs

(Top panel) In the absence of E2, ER exists as a monomer and dissociates from SRCs and KDM4B. (2nd panel) In the presence of E2, E2-bound dimeric ER forms a complex with KDM4B and SRCs in Fbxo22-positive breast cancer cells. This complex formation activates ER signaling. (3rd panel) In the presence of SERMs, SCF^{Fbxo22} specifically ubiquitylates KDM4B complexed with SERM-bound ER for degradation. KDM4B degradation in turn accelerates the dissociation of SRCs from ER and association between ER and N-CoR in Fbxo22-positive breast cancer cells. The dissociation of the complex inactivates ER signaling. (Bottom panel) In the presence of SERMs, SERM-bound ER still associates with SRCs and KDM4B through its AF1 domain in Fbxo22-negative cells. The resultant complex activates ER signaling.

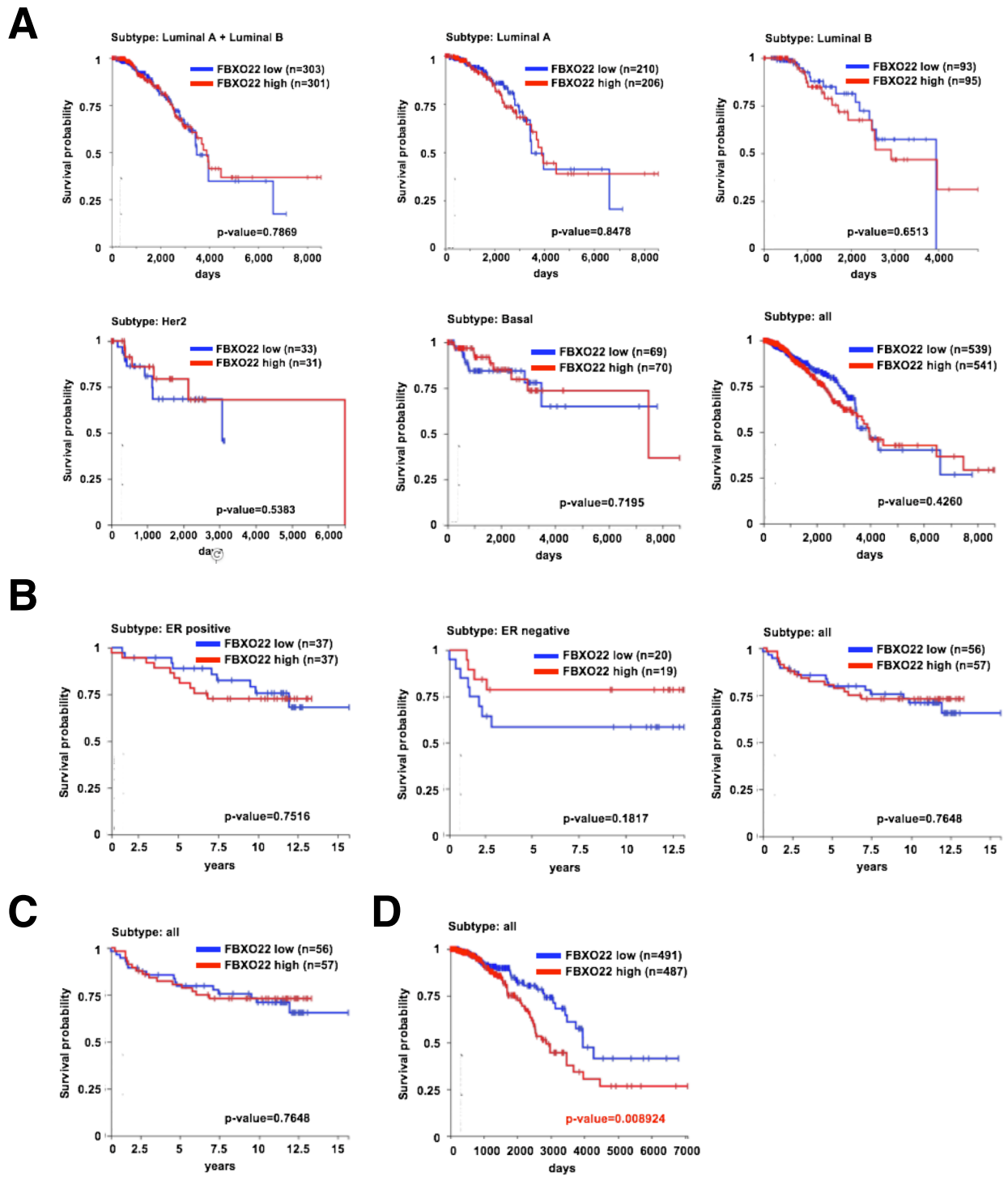

Supplementary Figure 14. Low Fbxo22 at the gene expression level does not associate with a poor outcome in patients with breast cancers in online databases. Overall survival stratified by the Fbxo22 gene expression level in indicated subtypes of breast cancer in TCGA **(A),** Breast Cancer (Caldas 2007) **(B)**, ICGC (specimen centric)**(C)** and ICGC (US donor centric)**(D)** data bases downloaded using the UCSC Xena browser (http://xena.ucsc.edu/).

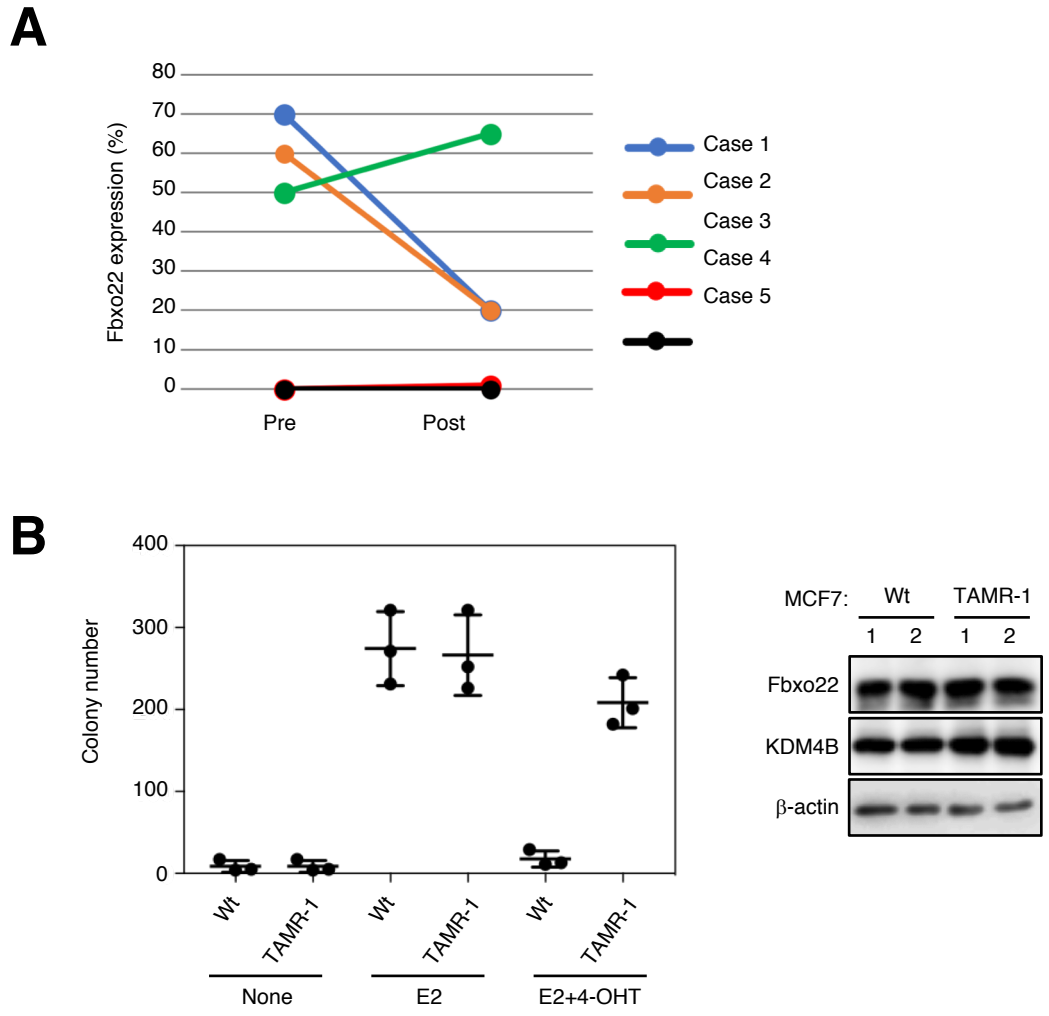

Supplementary Figure 15. The expression levels of Fbxo22 and KDM4B did not vary in ER-positive breast cancers pre and post treatment with neoadjuvant hormone therapy, and in TAM sensitive and resistant MCF-7 cells

(A) The expression levels of Fbxo22 did not vary in ER-positive/HER2-negative breast cancers pre and post treatment with neoadjuvant hormone therapy. Five patients who underwent the therapy were additionally examined for Fbxo22 expression with surgical specimens. Whereas three Fbxo22-positive cases (Cases 1, 2 and 3) remained positive after the therapy, two Fbxo22-negative cases (Cases 4 and 5) remained virtually negative (0% for Case 1 and 1% for Case 2). **(B)** TAM sensitive (Wt) and resistant (TAMR-1) MCF-7 cells established after a long term treatment with TAM (purchased form ATCC) were starved of E2, treated with E2 (10 nM) in the presence or absence of 4-OHT (100 nM) for 6 hrs, and then subjected to a quantitative colony formation assay. The results (left panel) are shown as the means ±s.d. of three independent experiments. The lysates from each of two independent clones were subjected to immunoblotting using the indicated antibodies.

A

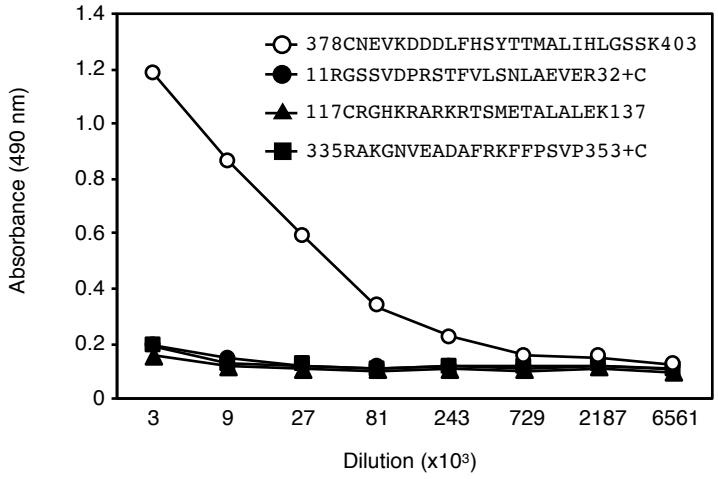

B

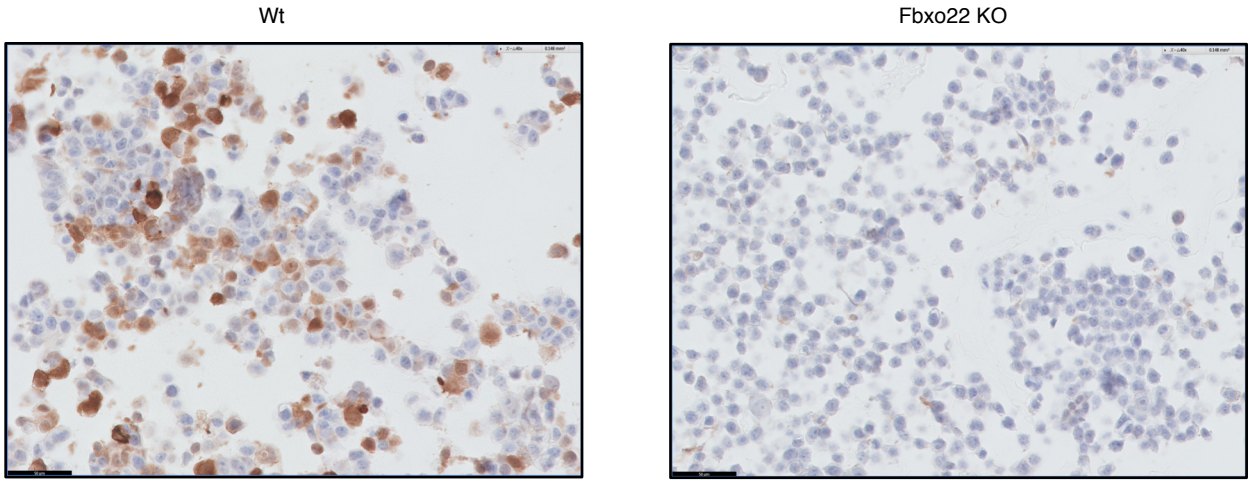

Supplementary Figure 16. Specificity of anti-Fbxo22 monoclonal antibody (FO22)

(A) Specificity of antibodies to Fbxo22 was evaluated by ELISA using peptides as indicated. **(B)** Pellets prepared from Wild-type (Wt) or Fbxo22 KO (Fbxo22 KO) MCF-7 cells were formalin-fixed, paraffin-embedded, and subjected to immunohistochemical analysis using Fo-22 monoclonal antibody (in the same fashion as for the tissue immunohistochemistry).

Supplementary Table 1. Distribution of Clinicopathological Characteristics

Characteristics	Fbxo22 expression		*P*
	positive	negative	
Total samples	114	49	
Age, years			
Mean	56	54	
SD	13	13	0.4036[3)]
Node			
Positive	60	27	
Negative	54	22	0.7719[4)]
Grade			
Low	67	24	
Medium / High	47	25	0.2483[4)]
Histology[1)]			
IC of NST (invasive ductal)	95	35	
Invasive lobular Ca	4	7	
Mucinous Ca	8	2	
Ca with apocrine differentiation	3	0	
Others	4	5	0.02797[5)]
PR[2)]			
Positive	95	33	
Negative	19	16	0.0227[4)]
Ki67[2)]			
high	28	24	
low	86	25	0.0022[4)]
Chemotherapy			
No	52	17	
Yes	62	32	0.1957[4)]
Hormone therapy			
No	3	2	
tamoxifen	32	14	
aromatase inhibitors	59	23	
both (TAM & AI)	18	10	
Others	2	0	0.8386[5)]

1) Histology was determined based on WHO 2012 classification
IC of NST: invasive carcinoma of no special type
2) PR status: 0% vs 1%≦, Ki-67 status: ≦ 10% vs 20%≦
3) unpaired t-test
4) Chi-square test
5) Fisher's exact test

Supplementary Table 2. Association between Fbxo22 positivity or clinical variables and relapse free survival

	Univariate			Multivariate		
Variable	HR	95% CI	*P*	HR	95% CI	*P*
Fbxo22						
Positive	1.00			1.00		
Negative	2.847	1.248 to 6.493	0.0129	2.6483	1.1148 to 6.291	0.0274
Node						
Negative	1.00			1.00		
Positive	1.639	0.6936 to 3.872	0.26	1.5679	0.6520 to 3.771	0.3151
Grade						
Low	1.00			1.00		
Medium / High	1.651	0.7231 to 3.768	0.234	1.4838	0.6396 to 3.442	0.3581
PR						
Negative	1.00			1.00		
Positive	0.7585	0.2983 to 1.929	0.562	0.8473	0.3257 to 2.204	0.7341
Ki67						
Negative	1.00			1.00		
Positive	1.54	0.6656 to 3.562	0.313	1.0409	0.4293 to 2.524	0.9293

* Estimated from Cox proportional hazards model.

Supplementary Table 3. Distribution of Clinicopathological Characteristics in the validation cohort

Characteristic	Fbxo22 expression		*P*
	positive	negative	
Total samples	13	17	
Age, years			
Mean	55	56	
SD	16	14	0.892 [3]
Node			
Positive	4	6	
Negative	9	11	0.795 [4]
Grade			
Low	9	9	
Medium / High	2	7	0.166 [4]
Histology [1]			
IC of NST (invasive ductal)	8	16	
Invasive lobular Ca	0	1	
Mucinous Ca	5	0	0.009 [5]
PR [2]			
Positive	11	13	
Negative	2	4	0.581 [4]
Ki67 [2]			
high	7	12	
low	6	5	0.346 [4]
Chemotherapy			
No	9	9	
Yes	4	8	0.367 [4]
Hormone therapy			
No	1	3	
tamoxifen	7	6	
aromatase inhibitors	5	8	0.680 [5]

1) Histology was determnined based on WHO 2012 classification
IC of NST: invasive carcinoma of no special type
2) PR status: 0% vs 1%≦, Ki67 status: ≦ 10% vs 15%≦
3) unpaired t-test
4) Chi-square test
5) Fisher's exact test

Supplementary Table 4. Distribution of Clinicopathological Characteristics of ER-negative breast cancer cohort

Characteristic	Fbxo22 expression		*P*
	high	low	
Total samples	20	21	
Age, years			
Mean	58	55	
SD	10	16	0.445[3)]
Node			
Positive	9	5	
Negative	11	16	0.1526[4)]
Grade			
Low	6	2	
Medium / High	14	19	0.09818[4)]
Histology[1)]			
IC of NST (invasive ductal)	16	17	
Invasive lobular Ca	1	1	
Ca with apocrine differentiation	2	0	
Others	1	3	0.5684[5)]
PR[2)]			
Positive	0	0	
Negative	20	21	NA
Ki67[2)]			
high	14	19	
low	6	2	0.09818[4)]
Chemotherapy			
No	1	7	
Yes	19	14	0.02212[4)]

1) Histology was determnined based on WHO 2012 classification
IC of NST: invasive carcinoma of no special type
2) PR status: 0% vs 1%≦, Ki67 status: ≦ 10% vs 15%≦
3) unpaired t-test
4) Chi-square test
5) Fisher's exact test

Supplementary Table 5. shRNA sequences used in this study

Target gene	Sequence	Reference	Type
Fbxo22	GGAATTGTAGTGACTCCAATG	(Johmura et al., 2016)	lentivirus
KDM4B	GGAAGGACATGGTCAAGAT	(Kawazu et al., 2011)	lentivirus
Luciferase	CGTACGCGGAATACTTCGA	(Elbashir et al., 2001)	lentivirus

Supplementary Table 6. Antibodies used in this study

Antibodies	Species	Source
Anti-alpha-beta-Actin (DMIA+BMIB)	Mouse	Neomarkers, Fremont, CA
Anti-beta-Actin (6276)	Mouse	Abcam, Cambridge, United Kingdom
Anti-ERalpha (D8H8)	Rabbit	Cell Signaling Technology, Boston, MA
Anti-ERalpha (HC-20)	Rabbit	Santa Cruz Biotechnologies, Santa Cruz, CA
Anti-ERalpha (H-184)	Rabbit	Santa Cruz Biotechnologies, Santa Cruz, CA
Anti-Fbxo22 (N3C3)	Rabbit	GeneTex, Irvine, CA
Anti-Fbxo22 (FF-7)	Mouse	Santa Cruz Biotechnologies, Santa Cruz, CA
Anti-Fbxo22	Mouse	In this study
Anti-FLAG (M2)	Mouse	Sigma, St. Louis, MO
Anti-HA (3F10)	Rat	Roche, Basel, Switzerland
Anti-HA (12CA5)	Mouse	Boehringer, Mannheim, Germany
Anti-HDAC3 (7G6G5)	Rabbit	Cell Signaling Technology, Boston, MA
Anti-KDM4A (N154/32)	Mouse	UC Davis/NIH NeuroMab Facility, Davis, CA
Anti-KDM4B (D7E6)	Rabbit	Cell Signaling Technology, Boston, MA
Anti-KDM4C (27532)	Rabbit	Abcam, Cambridge, United Kingdom
Anti-KDM4D (63199)	Rabbit	Abcam, Cambridge, United Kingdom
Anti-NcoR (5948)	Rabbit	Cell Signaling Technology, Boston, MA
Anti-p300 (D2X6N)	Rabbit	Cell Signaling Technology, Boston, MA
Anti-SRC3 (5E11)	Rabbit	Cell Signaling Technology, Boston, MA
Anti-StrepII (PAB16603)	Rabbit	Abnova, Walnut, CA
Anti-Tubulin	Rabbit	Cell Signaling Technology, Boston, MA

Supplementary Table 7. Primer sequences used in this study

Target gene	Sequence	Experiment type
EBAG9-Fw	TCCCACCTTCCTTTCGC	qPCR
EBAG9-Rv	CCAGTCGCAGTTTCCTCAC	qPCR
GREB1-Fw	GTGGTAGCCGAGTGGACAAT	qPCR
GREB1-Rv	AAACCCGTCTGTGGTACAGC	qPCR
KDM4B-Fw	GATGGCTCCTACAGCGACAA	qPCR
KDM4B-Rv	GTCCCTACTCGTGATGCTCTC	qPCR
MYB-Fw	GAAAGCGTCACTTGGGAAAA	qPCR
MYB-Rv	TGTTCGATTCGGGAGATAATTGG	qPCR
TFF1-Fw	TTGTGGTTTTCCTGGTGTCA	qPCR
TFF1-Rv	TCGAAACAGCAGCCCTTATT	qPCR